JOURNAL OF MATERIALS SCIENCE 10 (1975) 683–691

An examination of tellurium ion-implanted GaAs by transmission electron microscopy

B. J. SEALY*
Department of Physics, University of Surrey, Guildford, Surrey, UK

The effect of implanting high energy tellurium ions into single crystal GaAs has been investigated by transmission electron microscopy. Results from annealing experiments on specimens implanted at room temperature show that two anneal stages centred near 200 and 600° C occur, the actual anneal temperature being dose dependent. Non-crystalline surface layers were formed after implanting doses in the range 5×10^{13} to 5×10^{15} ions cm^{-2} at room temperature. However, implanting similar doses at 180° C caused no change in crystallinity. Thus the low temperature anneal stage which is the epitaxial recrystallization of the non-crystalline material, does not occur for the higher implant temperature. The high temperature anneal stage is associated with the annealing out of tiny defects such as twins and/or stacking faults leaving a single crystal containing only dislocation loops. The anneal stages observed by electron microscopy correlate with changes in sheet resistivity and Rutherford backscattering measurements on similar material. It is suggested that changes in dislocation loop size and density at high temperatures are coincident with the attainment of electrical activity.

1. Introduction

The role of tellurium in GaAs is not well understood even though a number of publications have discussed this system in detail. Ion implantation creates additional parameters and concepts which make the situation even more complex. Various methods have been used to investigate the processes that occur in ion-implanted GaAs but little use has been made of transmission electron microscopy (TEM). However, the value of TEM has been demonstrated for implanted GaAs [1, 2] and results have shown that gross lattice damage, that is, amorphization, occurs for high doses of ions implanted at room temperature. Subsequent annealing at low temperatures ($\sim$ 200° C) causes recrystallization of the damage and the formation of a twinned structure [2].

A major problem in the case of tellurium ions implanted into GaAs and annealed above 600° C is that only a few percent of the implanted ions become electrically active, this activity normally being at a depth beyond the range of the majority of implanted ions [3]. In order to investigate this problem we have implanted high doses (5×10^{13} to 5×10^{15} ions cm^{-2}) of tellurium ions into GaAs to look for trends in observable parameters as a function of ion dose, anneal temperature and implant temperature. The TEM results have been compared with published electrical measurements and Rutherford backscattering studies (RBS) of ion implanted GaAs.

2. Experimental

(1 1 0) oriented slices, about 1 mm thick were cut from bulk-grown tellurium-doped GaAs supplied by Mining and Chemical Products Ltd, given a free etch to remove saw damage, and then polished on one side using a 3% Br in methanol solution. Following a final free etch to remove residual damage, the specimens were implanted with tellurium ions incident at about 7° to the surface normal in order to prevent ion channelling. After implantation, specimens were cut into 2.2 mm diameter discs using an ultrasonic drill, followed by jet-etching from the back, unpolished, unimplanted face until perforation. The thinned specimens were washed thoroughly in acetone and absolute alcohol, dried on clean filter paper and mounted in the high tilt goniometer stage of a Jeol JEM 120 electron microscope operating at an accelerating voltage of 120 kV.

In order to make the tellurium ion electrically

* Present address: Department of Electrical and Electronic Engineering, University of Surrey, Guildford, Surrey.

active, a post-implantation anneal is required at a temperature of at least 600°C [3]. Thus isochronal anneals (15 min) were carried out at temperatures up to 750°C in flowing nitrogen at atmospheric pressure. At the higher anneal temperatures (> 600°C) severe pitting and surface degradation occur accompanied by changes in non-stoichiometry. Thus the implanted surface was protected with about 3000 Å of SiO_2 deposited by the pyrolytic oxidation of silane [4]. After annealing, the SiO_2 was removed by washing the specimens for 1 min in a solution of HF + H_2O in the ratio 1:1 by volume. This treatment left a clean, highly polished surface with no trace of SiO_2 as estimated by TEM, by electron spectroscopy (ESCA) [4], and by Rutherford backscattering experiments [4]. Following the anneal and removal of the encapsulant, the specimens were prepared for observation by TEM.

3. Results

3.1. Room temperature implants

The observations fall into three approximate anneal temperature ranges (1) RT to 250°C, (2) 250 to 600°C and (3) 600 to 750°C, each of which will be considered in turn (see Table I).

3.1.1. RT to 250°C

Ion doses in the range 5×10^{13} to 5×10^{15} ions cm^{-2} were found to produce gross lattice damage in the form of a continuous amorphous layer which recrystallized epitaxially on annealing. Appreciable recrystallization occurred after annealing in the range 130 to 200°C but there still remained a strong diffuse ring pattern. There was evidence from TED that recrystallization occurred from the surface as well as the substrate, since if the electron beam initially passed through the implanted layer, double diffraction was apparent. (Fig. 1). Thus there must be an ordered crystalline surface layer sandwiching the damaged amorphous material between the substrate and surface even after high dose implants at 150 keV.

During recrystallization at 200°C, a fine granular spotty contrast effect was observed which became coarser with increasing anneal temperature and which still remained after annealing at high temperatures ($\gtrsim$ 600°C) (see Fig. 2a to c).

After annealing at 250°C a single crystal (1 1 0) diffraction pattern formed and no trace of the amorphous phase remained. The ⟨1 1 1⟩

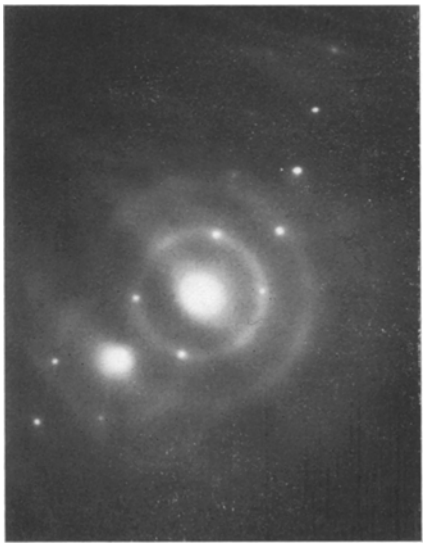

Figure 1 Diffraction pattern of unannealed GaAs implanted at room temperature with 2.5×10^{15} Te^+ ions cm^{-2} at 150 keV showing the effects of double diffraction through a single crystal surface layer, $\mathbf{g} = [2\bar{2}0]$.

streaks and additional spots at $\frac{1}{3}$ ⟨1 1 1⟩ are consistent with twinning/stacking faults on {1 1 1} planes (Fig. 2d). We thus suggest that the granularity could represent these defects. At this temperature (250°C) patches of Moiré fringes also formed (Fig. 2a). We will refer to the stacking faults, twins and Moirés collectively as "disorder" in the following paragraphs.

3.1.2. 250 to 600°C

The average separation of the observed Moiré fringes increased by about 50% in this temperature range which is indicative of a gradual realignment of misoriented material. It was found that under two beam conditions, many fringes were parallel to the operating vector direction which suggested that the Moirés were mainly rotational, that is, in general, they resulted from small angular rotations about the normal to the foil surface and not from differences in lattice spacings. Thus they most likely form because of double diffraction between epitaxial material and crystallites, which have nucleated in the damaged region and have not grown epitaxially. From the mean spacing of the Moiré fringes we compute that the rotational misorientation decreases from about 2° to less than about 1° over the anneal temperature range 250 to 600°C.

Using thickness contours as a guide, it was

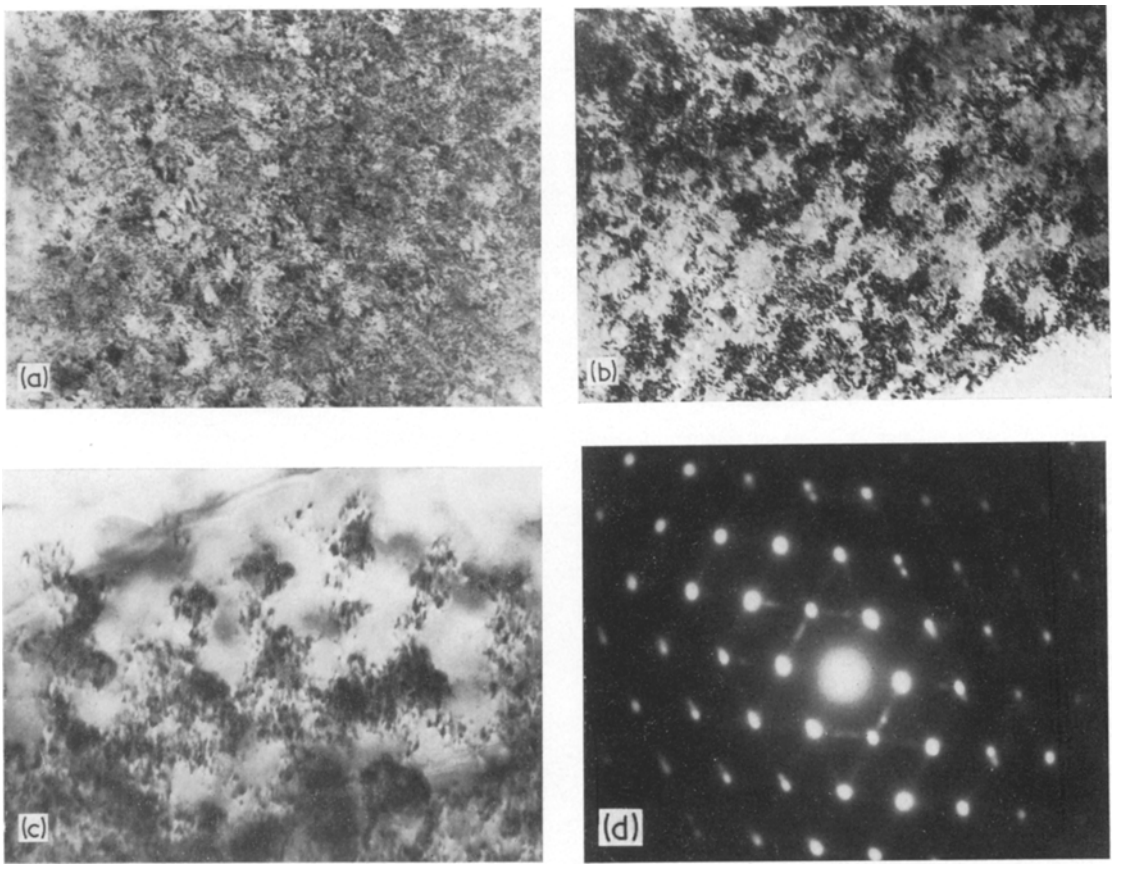

Figure 2 GaAs implanted at room temperature with 2.5×10^{15} Te^+ ions cm^{-2} at 150 keV. (a) $T_a = 260°C$, diffraction pattern for this micrograph is similar to (d), × 72 000. (b) $T_a = 490°C$, $\mathbf{g} = [2\bar{2}0]$, × 72 000. (c) $T_a = 375°C$, $\mathbf{g} = [1\bar{1}1]$, × 72 000. (d) Typical diffraction pattern for a recrystallized specimen for $T_a = 260°C$, showing $\langle 1\bar{1}1 \rangle$ streaks, extra spots at $\frac{1}{3}\langle 1\bar{1}1 \rangle$ and $\frac{2}{3}\langle 1\bar{1}1 \rangle$ and spot splitting in $\langle 002 \rangle$ directions.

discovered that approximately the first few 100 Å from the implanted surface was devoid of "disorder". For thicker regions of specimens with a low taper angle (so that the foil thickness increased slowly with distance from the edge of the jet-etched hole) the disordered regions were seen to occupy small areas isolated from one another. These regions overlapped at thicker parts of the specimen and thus must occur at varying depths in the crystal (Fig. 2b).

3.1.3. 600 to 750° C

In this temperature range, the "disorder" annealed out and dislocation loops appeared at approximately the same depth from the implanted surface. Small loops about 100 to 300 Å diameter appeared after annealing for 15 min. at 570° C in specimens implanted with 5×10^{13} Te^+ ions cm^{-2} but "disorder" was still present for specimens implanted with 2.5×10^{15} Te^+ ions cm^{-2} and annealed at 650° C for 15 min. Thus the formation of loops is dose dependent.

There appeared to be an intermediate stage where the Moiré fringes and granularity had annealed out and small linear defects (dislocations?) and small dislocation loops formed (Fig. 3a). At slightly higher temperatures the linear defects disappeared leaving only loops which had grown in size during this anneal (Fig. 3b). A specimen implanted with a dose of 1×10^{15} ions cm^{-2} and annealed at 570° C showed a depth dependence of disorder (Fig. 4a). At the surface there was little visible "damage" but a pale, patchy contrast effect was observed which could be the result of uneven etching. Deeper, but still near the surface (say 100 to 200 Å) small lines

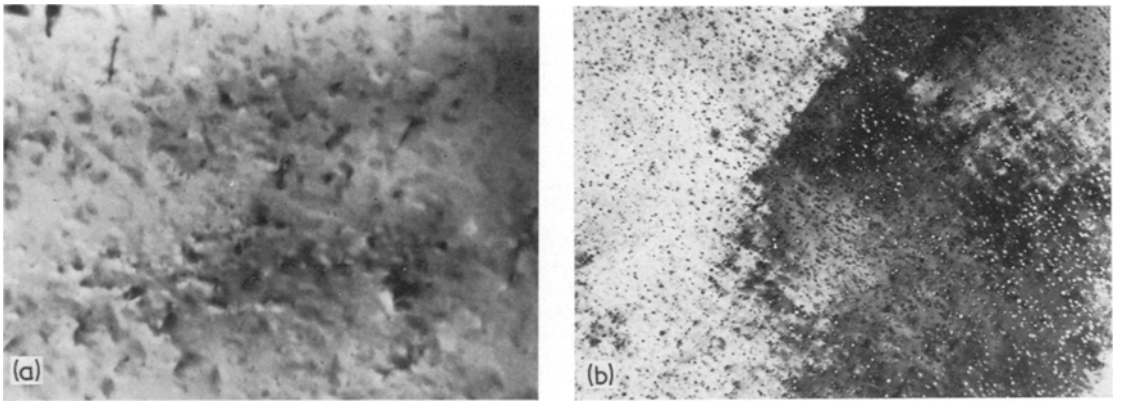

Figure 3 GaAs implanted at room temperature with 5×10^{13} Te^+ ions cm^{-2} at 150 keV, g = [1$\bar{1}$3]. (a) T_a = 570°C, × 45 000, (b) T_a = 610°C, × 23 000.

and loops were found whereas Moiré fringes appeared beyond this depth (see also Fig. 4b). This observation must be related to the dose dependence of the anneal stage since the dose near the surface was estimated to be about 10^{14} ions cm^{-2}. Thus we suggest that for doses in the range 5×10^{13} to 5×10^{15} ions cm^{-2} the change from "disorder" to loops begins near 570°C but the width of the anneal stage depends on the implanted dose.

The size and density of loops has been estimated for many specimens but no obvious correlation between these parameters and the implant conditions was found. The range of loop sizes was similar for specimens implanted with a dose of 5×10^{13} ions cm^{-2} or 2.5×10^{15} ions cm^{-2} (Fig. 5). However, a few percent of the loops in the higher dose specimens sometimes had diameters up to about 1300 Å.

3.2. 180°C implants

A limited number of specimens were implanted with 1×10^{15} Te^+ ions cm^{-2} at 180°C (implant energy = 150 keV). In this case no surface amorphization occurred and no observable defects were found in unannealed specimens in agreement with published data [1, 2]. However, annealing at temperatures in the range 590 to 750°C produced specimens which were quite unlike any heat-treated specimens which had been implanted at room temperature. For example, after annealing at 600°C, very large non-circular loops were found (Fig. 4c). When only the large loops are considered, it is observed (Fig. 4c) that many circular loops greater than about 1000 Å diameter appear to lie in the plane of the foil, that is, lie on the (1 1 0) plane. The direction of the major axis of many elliptical loops is such as to suggest these may lie on inclined {1 1 0} planes. This is consistent with the loops being circular and of diameter about 2400 Å. However, some loops must be truly ellipsoidal with major axes up to 5000 Å long and possibly were formed by the coalescence of adjacent loops (Fig. 4c).

There is a second distribution of loop sizes with mean diameter about 120 Å whose density is about an order of magnitude larger than the very large loops (Fig. 5) and many of which lie nearer to the implanted surface than the large loops. This is evidenced by the fact that only small loops are seen in the thinner parts near the specimen edge (Fig. 4c).

Annealing at 750°C caused an increase in the size of the smaller loops but no "wavy" loops were found (cf. Fig. 4c and d). Evidence for two distributions of loop sizes was obtained after annealing at 750°C but was not so apparent as for specimens annealed at 600°C (Fig. 5).

3.3. Precipitation

The published phase diagram for the Te–GaAs ternary [5] together with electrical measurements [6, 7] on tellurium-saturated GaAs as a function of anneal temperature suggest that tellurium has a retrograde solubility in GaAs and a maximum donor concentration of about 10^{19} cm^{-3} occurring near 1100°C. In an attempt to observe precipitation in ion implanted GaAs the tellurium ion dose was increased to 5×10^{15}

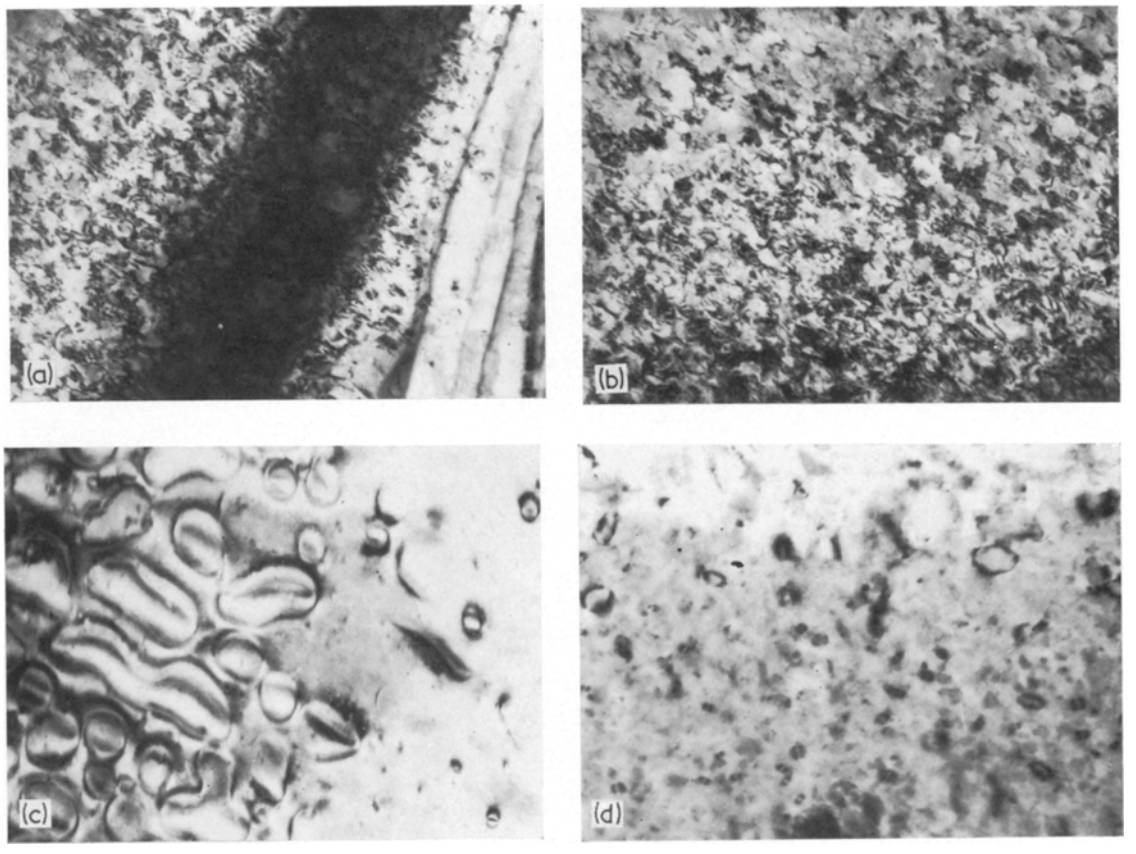

Figure 4 GaAs implanted with 1×10^{15} Te^+ ions cm^{-2} at 150 keV. (a) and (b) $\mathbf{g} = [2\bar{2}0]$, $T_a = 570°C$, $\times$ 45 000, room temperature implant, (a) near an edge showing first extinction contour. (c) $\mathbf{g} = [3\bar{3}3]$, $T_i = 180°C$, $T_a = 600°C$, $\times$ 72 000, near an edge, (d) $\mathbf{g} = [2\bar{2}0]$, $T_i = 180°C$, $T_a = 750°C$, $\times$ 72 000, also showing patches of β–Ga_2O_3 on the surface.

ions cm^{-2}. The ion range was small due to the low implant energy of 50 keV so that the peak of the Gaussian distribution was close to the surface (170 Å) with a peak tellurium concentration of about 6 at. % which is far in excess of the estimated solid solubility [6]. After annealing at 600 or 750° C for 15 min, specimens were found to be of single crystal form, to contain dislocation lines but showed no evidence for Te or Ga_2Te_3 precipitates. Unfortunately, a complicating factor was the formation of β–Ga_2O_3 at the SiO_2–GaAs interface during the anneal [4]. Stereo microscopy indicated that the oxide penetrated into the GaAs to a depth approximately equal to that of the dislocations below the implanted surface, that is about 100 to 200 Å. The chemical composition depth profiles of similar specimens analysed using electron spectroscopy (ESCA) confirmed the above observation [4]. Thus the formation of an oxide could mask the observation of Te or Ga_2Te_3 precipitates for low energy implants and make difficult the interpretation of diffraction patterns since many β–Ga_2O_3, Te and Ga_2Te_3 lines overlap.

Selected-area diffraction from specimens containing a high density of large loops showed no lines or spots due to Te or Ga_2Te_3. We thus infer that if precipitates do form in implanted material (1) the concentration is low, (2) they are extremely small, (3) they are homogeneously distributed throughout the lattice, and (4) the dislocation loops formed after high temperature anneals are unlikely to be precipitates of Te or Ga_2Te_3.

4. Discussion

4.1. Correlation of anneal stages with electrical and RBS measurements

For material implanted at room temperature, two anneal stages have been identified and are

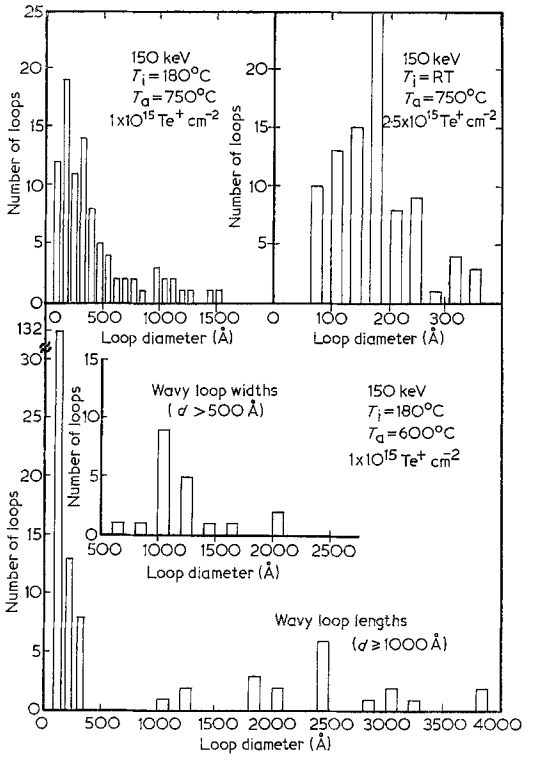

Figure 5 Histograms of dislocation loop diameters for Te^+ ion-implanted GaAs after annealing.

(a) the amorphous to crystalline transition at 200 to 250° C and (b) loop formation at temperatures above about 570° C. RBS measurements of lattice disorder show a marked decrease near 100 to 200° C for 6.5 × 10^{13} cm^{-2} of 40 keV Te^+ ions and a similar percentage decrease for 7 × 10^{15} Te^+ ions cm^{-2} but at a slightly higher temperature between 200 to 300° C [8]. Both correlate with a broad minimum in sheet resistivity as a function of anneal temperature [3]. Thus both RBS and sheet resistivity measurements indicate a significant change in properties which TEM results confirm and show to be the epitaxial recrystallization of the amorphous layer produced during implantation. This low temperature anneal stage has been observed previously by TEM in specimens bombarded with neon [1] and argon [2] ions, the former recrystallizing between 270 and 300° C and the latter between 120 and 150° C. The latter reference included a preliminary study of the implantation of tellurium ions and showed that they behaved in a similar way to argon ions but the anneal temperature dependence could be different [2]. Thus the range of recrystallization temperatures appears to be due both to a dose dependence and to differences in ion mass. For tellurium ion doses between 5 × 10^{13} ions cm^{-2} and 5 × 10^{15} ions cm^{-2} it is suggested that recrystallization occurs > 150° C for the lower dose and < 250° C for the higher dose. An anneal stage at about 250° C has also been observed for high doses of 1 MeV zinc ions [9] and 1 MeV electrons [10] implanted into GaAs at room temperature.

Following recrystallization, an increase in anneal temperature caused a continued decrease in disorder as estimated from RBS measurements. For example, a dose of 1 × 10^{15} cm^{-2} of 40 keV Te^+ ions produced a decrease in disorder from about 50% to less than 10% over the temperature range 300 to 550° C [8]. However, measurements of sheet resistivity indicated a sharp increase with increasing anneal temperature over this temperature range for specimens implanted with 5 × 10^{14} cm^{-2} of 150 keV Te^+ ions at room temperature [3]. The TEM results suggest that lattice disorder becomes minimal when the Moirés, twins and stacking faults anneal leaving only loops. The temperature at which this occurs is dose dependent and for a tellurium dose near 5 × 10^{14} ions cm^{-2} is likely to occur for anneal temperatures greater than about 600° C (Table I). After annealing at about 640° C, the difference between the number of tellurium ions residing on or close by lattice sites [3] after 180° C (90%) or room temperature (45%) implants suggests that the latter, low degree of occupancy of lattice sites by tellurium is due to appreciable "damage" still being present and thus must be dose dependent. Hence, once loops are formed, more than about 90% of the implanted tellurium should occupy lattice sites.

Our results for 1 × 10^{15} Te^+ ions cm^{-2} implanted at 180° C show a decrease in loop density from 8 × 10^{10} cm^{-2} to 6.4 × 10^9 cm^{-2} after annealing at 600 and 750° C respectively. This is in accord with published data for argon ions implanted into GaAs at 100° C followed by annealing at 700 or 800° C [2]. In contrast, specimens implanted with doses greater than about 2.5 × 10^{15} ions cm^{-2} at room temperature did not form loops till annealed in the range 650 to 750° C (Table I). A change in loop density was not established for these specimens even at 750° C which was the highest anneal temperature. These observations correlate with the attainment of donor activity which is observed in room temperature implanted specimens only after

TABLE I Summary of anneal behaviour as a function of ion dose for specimens implanted at room temperature

Anneal temperature (°C)	Dose (ions cm^{-2})	Observation
As-implanted	5×10^{13}	Non-crystalline
As-implanted	5×10^{15}	Non-crystalline
130	5×10^{13}	Non-crystalline + granular defects
130	2.5×10^{15}	Non-crystalline + granular defects
175	2.5×10^{15}	Non-crystalline + granular defects
200	2.5×10^{15}	Non-crystalline + granular defects
250	2.5×10^{15}	Disorder
400	2.5×10^{15}	Disorder
500	5×10^{13}	Disorder
500	2.5×10^{15}	Disorder, little oxide
570	5×10^{13}	Few very small loops, dislocation lines, oxide
570	1×10^{15}	Disorder, tiny black/white spots (loops?)
570	2.5×10^{15}	Disorder, oxide
600	5×10^{13}	Many loops, oxide
600	2.5×10^{15}	Disorder, oxide, (loops?)
600	5×10^{15}	Disorder, oxide, (loops?) dislocation lines
650	2.5×10^{15}	Disorder, oxide
740	2.5×10^{15}	Loops, oxide
740	5×10^{15}	Loops (?), oxide

Note that "disorder" refers to the presence of Moirés, twins/stacking faults and granular defects.

TABLE II High temperature anneal stage in room temperature implanted GaAs

Anneal stage (°C)		Implant details			Ref.
T (ρ_s(max))	T (ρ_s(min))	Ion	Energy (keV)	Dose range (ions cm^{-2})	
400	$\gtrsim$600	Zn^+	60	1×10^{12}–3×10^{14}	[11]*
400-450	~650	Zn^+	30	1×10^{14}–4×10^{15}	[12]*
$\lesssim$650	800*†	Zn^+	1000	1–5 $\times 10^{14}$	[9]*‡
$\lesssim$600	~800	Zn^+	20	1×10^{13}–1×10^{15}	[13]†*
$\lesssim$600	~800	Cd^+	60	1×10^{13}–1×10^{15}	[13]†*
$\lesssim$600	~800	S^+	100	1×10^{13}–1×10^{15}	[13]†*
500-600	~800	S^+	150	1×10^{15}	[14]*
$\approx$600	—	N^+	200	5×10^{14}	[14]*
500-600	~700	Si^+	50, 10	5×10^{13}–1×10^{15}	[15]*
~500	—	Te^+	40	6.5×10^{13}, 1×10^{15}	[8]†
$\gtrsim$550	~800	Te^+	60,150	5×10^{14}	[3]*
$\gtrsim$550	—	Cd^+	60, 150	5×10^{14}	[3]*
$\lesssim$600	~800	Cd^+	5, 10, 25, 60	8×10^{14}	[16]*
400-700	>750	Cd^+	20, 40	5×10^{13}–1×10^{16}	[17]†
~600	—	S^+	30	5×10^{14}	[18]§*
~600	—	Se^+	30	5×10^{14}	[18]§*
~600	—	Te^+	30	5×10^{14}	[18]§*
500	~800	Ge^+	30	4×10^{15}	[19]§*

*Sheet resistivity measurements, ρ_s.
†R.B.S. measurements.
‡Implant temperature = 77 K.
§Implant temperature = 300°C.

annealing to about 800°C, similar activity occurring in 180°C implanted specimens near 650°C [3]. Published data indicate a maximum in sheet resistivity versus anneal temperature near 600°C for various implanted dopants in GaAs (Table II) and is due to acceptor like lattice defect annealing for $T_a < 500$°C and to implanted dopant activity for $T_a \gg 500$°C [3].

Thus loops are formed near the temperature at which the maximum in sheet resistivity versus anneal temperature occurs and the change in loop density and size correlates with the decrease in sheet resistivity with increasing anneal temperature. Published data also indicate that the decrease in sheet resistivity at high temperatures (Table II) is coincident with an increase in both electrical activity and Hall mobility [3, 9].

4.2. Precipitation

Although the presence of precipitates was not confirmed, one can speculate that if stacking faults are present they may be extrinsic in accord with published data [20]. Thus the small percentage (45%) of substitutional tellurium atoms found from RBS measurements in room temperature implanted specimens may be due to stacking faults containing Ga_2Te_3 or Te platelets. Precipitates of probable composition Ga_2Te_3 or Ga_2Se_3 have been observed by TEM in tellurium [21] and selenium [22] saturated GaAs, respectively. However, detailed annealing experiments on tellurium doped GaAs have indicated varying results, for example, the formation of tellurium molecules [6], the precipitation of tellurium [23] and the formation of neutral complexes such as ($V_{Ga}Te$) [24] or ($V_{Ga}Te_3$) [21, 25, 26]. The formation of ($V_{Ga}Te$) is consistent with the phase equilibria of GaAs [27] and credibility for the existence of ($V_{Ga}Te_3$) complexes exists [25, 28]. There are also published data which show that the GaAs–Ga_2Se_3 system forms a complete solid solution, that is, no miscibility gap exists [29], but similar work on the GaAs–Ga_2Te_3 system [5, 30] does not agree with this result. However, it has been suggested that extensive solid solutions of Ga_2Te_3 in GaAs exist and that equilibrium in the solid solution region occurs very slowly [30]. Thus it is possible that the reported data for the solubility of Ga_2Te_3 in GaAs are in error because equilibrium was not attained and that the two phase condition is due only to the fact that the diffusion rates were too low [30]. One now has an explanation for the ion implantation results since we may have very small, thin, extrinsic stacking faults which because of radiation enhanced diffusion equilibrate after small anneal times (15 min) in the temperature range 600 to 750°C. However, an alternative explanation is that ion implantation allows a metastable situation to occur in which tellurium is appreciably more soluble than in similarly doped bulk-grown crystals. This could be tested by examining implanted material which has been annealed to very high temperatures so that thermodynamic equilibrium was achieved. But this is a difficult experiment to accomplish without a suitable high temperature protective coating. A further consideration is that TEM studies of neon and argon implanted GaAs show similar defects to those reported here. Hence these defects observed by TEM could be a property of damaged (heavy ion bombarded) GaAs alone and may not depend on the implanted ion species. The results of Table II tend to give weight to this argument since irrespective of the implanted ion the maximum in sheet resistivity as a function of anneal temperature occurs approximately at the same anneal temperature.

5. Conclusions

Tellurium ion doses in the range 5×10^{13} to 5×10^{15} ions cm^{-2} implanted into GaAs at room temperature were found to create a uniform amorphous layer with a small amount of crystalline material remaining at the surface. Epitaxial recrystallization was complete after annealing at 250°C but much damage remained in the form of micro-twins and/or stacking faults and rotational disorder (Moiré fringes). These were replaced by dislocation loops when annealed in the range 570 to 750°C, the anneal temperature being dose dependent. The TEM results correlate with changes in sheet resistivity, the attainment of electrical activity and RBS measurements of disorder. Both room temperature and 180°C implanted specimens annealed above 600°C gave rise to a high density of dislocation loops. Precipitation of tellurium or Ga_2Te_3 was not observed. However, it is suggested that if stacking faults occur they could contain platelets of either Te or Ga_2Te_3 which dissolve on heat treatment. In this way we obtain apparently single phase material containing up to 6 at. % tellurium. The observed defects are also found in neon and argon implanted GaAs so may be unrelated to the implanted ion species. In order to further assist in the interpretation of electrical data, one may need to characterize the dislocation loops and the fine granular structure observed after annealing specimens implanted at room temperature.

Acknowledgements

I would like to thank Professor K. E. Puttick

for his interest in the work and for comments on the manuscript. Thanks are also due to Dr K. G. Stephens for useful comments, to Dr P. L. F. Hemment for invaluable advice and help during the course of the work, to Dr C. T. Foxon of Mullard Research Laboratories, Redhill for advice on building the jet-etching apparatus and for helpful comments and discussion, and to Dr R. Bicknell of Plessey Co Ltd, Towcester for discussion and comments on the micrographs. The author would finally like to acknowledge the financial support of the Science Research Council.

References

1. D. J. MAZEY and R. S. NELSON, *Rad. Effects* **1** (1969) 229.
2. R. BICKNELL, P. L. F. HEMMENT, E. C. BELL and J. E. TANSEY, *Phys. Stat. Sol.* (*a*) **12** (1972) K9.
3. E. C. BELL, A. E. GLACCUM, P. L. F. HEMMENT, K. G. STEPHENS and J. E. TANSEY, private communication, to be published.
4. E. C. BELL, A. E. GLACCUM, P. L. F. HEMMENT and B. J. SEALY, *Rad. Effects* **22** (1974) 253.
5. M. B. PANISH, *J. Electrochem. Soc.* **114** (1967) 91.
6. C. S. FULLER and K. B. WOLFSTIRN, *J. Appl. Phys.* **34** (1963) 2287.
7. M. G. MIL'VIDSKII, V. B. OSVENSKII, V. I. FISTUL, E. M. OMEL'YANOVSKII and S. P. GRISHINA, *Sov. Phys. Semicond.* **1** (1968) 813.
8. G. CARTER, W. A. GRANT, J. D. HASKELL and G. A. STEPHENS, *Rad. Effects* **6** (1970) 277.
9. A. GUIVARC'H, P. N. FAVENNEC and G. PELOUS, Proceedings of the Conference on Radiation Damage and Defects in Semiconductors, Reading (1972) p. 429.
10. A. H. KALMA, R. A. BERGER and R. A. CESENA, *ibid* (1972) p. 364.
11. M. A. LITTLEJOHN, J. R. HAUSER and L. K. MONTEITH, *Rad. Effects* **10** (1971) 185.
12. V. M. ZELEVINSKAYA, G. A. KACHURIN, N. B. PRIDACHIN and L. S. SMIRNOV, *Sov. Phys. Semicond.* **4** (1971) 1529.
13. R. G. HUNSPERGER and O. J. MARSH, *Rad. Effects* **6** (1970) 263.
14. Y. KATO, Y. SHIRAKI, T. SHIMADA and K. F. KOMATSUBARA, Proceedings of the Conference on Radiation Damage and Defects in Semiconductors, Reading (1972) p. 348.
15. J. D. SANSBURY and J. F. GIBBONS, *Rad. Effects* **6** (1970) 269.
16. T. AMBRIDGE and R. HECKINGBOTTOM, private communication.
17. J. J. GROB, A. GHITESCU and P. SIFFERT, Proceedings of the Conference on Ion Implantation in Semiconductors and other Materials, edited by B. L. Crowder, Yorktown Heights (1972).
18. V. M. ZELEVINSKAYA and G. A. KACHURIN, *Sov. Phys. Semicond.* **5** (1972) 1455.
19. V. M. ZELEVINSKAYA and G. A. KACHURIN, *ibid* **5** (1971) 1011.
20. D. LAISTER and G. M. JENKINS, *J. Mater. Sci.* **3** (1968) 584.
21. H. KRESSEL, F. Z. HAWRYLO, M. S. ABRAHAMS and C. J. BUIOCCHI, *J. Appl. Phys.* **39** (1968) 3139.
22. M. S. ABRAHAMS, C. J. BUIOCCHI and J. J. TIETJEN, *ibid* **38** (1967) 760.
23. E. S. MEIERAN, *ibid* **36** (1963) 2544.
24. C. J. HWANG, *ibid* **40** (1969) 4584.
25. L. J. VIELAND and I. KUDMAN, *J. Phys. Chem. Solids* **24** (1963) 437.
26. I. V. MITCHELL, J. W. MAYER, J. K. KUNG and W. G. SPITZER, *J. Appl. Phys.* **42** (1972) 3982.
27. R. M. LOGAN, *J. Phys. Chem. Solids* **32** (1971) 1755.
28. G. SCHOTTKY, *ibid* **27** (1966) 1721.
29. N. A. GORYUNOVA and V. S. GRIGOR'EVA, *Sov. Phys. Tech. Phys.* **26** (1956) 2094.
30. J. C. WOOLLEY and B. A. SMITH, *Proc. Phys. Soc.* (*Lond.*) **72** (1958) 867.

Received 22 July and accepted 21 October 1974.